Published online 17 June 2010 *Nucleic Acids Research, 2010, Vol. 38, No. 19* ***6803–6812***
doi:10.1093/nar/gkq551

A switch-on mechanism to activate maize ribosome-inactivating protein for targeting HIV-infected cells

Sue Ka-Yee Law[1], Rui-Rui Wang[2], Amanda Nga-Sze Mak[1], Kam-Bo Wong[1], Yong-Tang Zheng[2,*] and Pang-Chui Shaw[1,*]

[1]Department of Biochemistry and Centre for Protein Science and Crystallography, The Chinese University of Hong Kong, Shatin, N.T., Hong Kong and [2]Key Laboratory of Animal Models and Human Disease Mechanisms, Kunming Institute of Zoology, Chinese Academy of Sciences, Kunming 650223, China

Received May 3, 2010; Revised May 28, 2010; Accepted May 29, 2010

ABSTRACT

Maize ribosome-inactivating protein (RIP) is a plant toxin that inactivates eukaryotic ribosomes by depurinating a specific adenine residue at the α-sarcin/ricin loop of 28S rRNA. Maize RIP is first produced as a proenzyme with a 25-amino acid internal inactivation region on the protein surface. During germination, proteolytic removal of this internal inactivation region generates the active heterodimeric maize RIP with full *N*-glycosidase activity. This naturally occurring switch-on mechanism provides an opportunity for targeting the cytotoxin to pathogen-infected cells. Here, we report the addition of HIV-1 protease recognition sequences to the internal inactivation region and the activation of the maize RIP variants by HIV-1 protease *in vitro* and in HIV-infected cells. Among the variants generated, two were cleaved efficiently by HIV-1 protease. The HIV-1 protease-activated variants showed enhanced *N*-glycosidase activity *in vivo* as compared to their un-activated counterparts. They also possessed potent inhibitory effect on p24 antigen production in human T cells infected by two HIV-1 strains. This switch-on strategy for activating the enzymatic activity of maize RIP in target cells provides a platform for combating pathogens with a specific protease.

INTRODUCTION

Ribosome-inactivating proteins (RIPs) are RNA *N*-glycosidases which cleave the *N*-glycosidic bond of adenine-4324 at the α-sarcin/ricin (SR) loop of 28S rRNA. The depurination of the SR loop results in the inhibition of protein synthesis by impairing the binding of EF-1 or EF-2 to the ribosomes, hence the high cytotoxicity of RIPs. Maize RIP is classified as a type III RIP. It is synthesized in the endosperm of maize as an inactive precursor, which contains a 25 amino acid internal inactivation region, 16 aa at the N-terminus and 14 aa at the C-terminus. During germination, a two-chain activated form is generated by endogenous proteolysis of the internal inactivation region, along with the removal of the N- and the C-terminal sequences. The two chains (16.5 and 8.5 kDa) are tightly associated without disulfide linkage. It has been shown that a variant (MOD) with the two chains fused through a 2 aa linker possessed protein inhibitory activity similar to that of the native two-chain form (1–3). Our group has solved the crystal structures of both MOD and a construct Pro-RIP which contains the 25 aa internal inactivation region but with the 16 aa N-terminal and 14 aa C-terminal sequences removed. We found that this internal inactivation region (Ala163–Asp189) is located on the surface of the N-terminal domain in Pro-RIP (4). The secondary structural elements of the crystal structure of MOD and its solution structure by nuclear magnetic resonance (NMR) spectrometry are comparable and most α-helices and β-strands are similar in length (5). Although maize RIP only has about 20% sequence homology with other type I and II RIPs, their *N*-glycosidase domains are similar and the active site residues including Tyr94, Tyr130, Glu207, Arg210 and Trp241 at the cleft between the N- and C-terminal are conserved (4–6). The presence of the internal inactivation region of maize RIP led us to derive a novel strategy to enhance the specificity of maize RIP towards target cells expressing a specific protease.

*To whom correspondence should be addressed. Tel: 852 26096803; Fax: 852 26037246; Email: pcshaw@cuhk.edu.hk
Correspondence may also be addressed to Yong-Tang Zheng. Tel/Fax: 86 0871 5195684; Email: zhengyt@mail.kiz.ac.cn

RIPs are highly cytotoxic and have been used as abortificiant (7,8), anti-cancer (9–11) and anti-HIV agents (12–17), either alone or as a component of immunotoxins (18,19). Many type I and II RIPs, such as MAP30, GAP30, DAP30, pokeweed antiviral protein (PAP) and ricin, have been reported to possess anti-HIV activity by inhibiting viral replication *in vitro* and *in vivo* (13,14,20–23), although the anti-HIV mechanism is still unclear. As a test case for increasing the specificity of maize RIP towards cells expressing a specific protease, we provide an account on the generation of HIV-1 protease-sensitive maize RIP by incorporating the HIV-1 protease recognition sequences to the internal inactivation region of the Pro-RIP (Figure 1). Several variants were constructed and two were found to be cleaved and activated by recombinant HIV-1 protease *in vitro* and in HIV-infected cells, resulting in an active two-chain form with *N*-glycosidase activity comparable to the fully active maize RIP. In addition, the variants inhibited viral replication in human T lymphocytes infected by two T-tropic HIV-1 strains, and their cytotoxicity towards uninfected cells was similar to the unactivated precursors.

MATERIALS AND METHODS

Construction, expression and purification of proteins

Maize [Δ1–16, Δ287–300]-Pro-RIP (Pro-RIP-WT) and [Δ1–16, Δ163–164, Δ167–189, Δ287–300]-Pro-RIP (MOD-WT) were provided by Prof. R.S. Boston. Pro-HIV-MA/CA-16, Pro-HIV-MA/CA-20, Pro-HIV-MA/CA, N-terminal TAT-fusion variants TAT-Pro-RIP, TAT-MOD, TAT-Pro-HIV-MA/CA-3aa, TAT-Pro-HIV-MA/CA-2aa, TAT-Pro-HIV-MA/CA and TAT-Pro-HIV-p2/NC were generated by polymerase chain reaction mutagenesis using overlapping primers and Phusion DNA polymerase (Finnzymes, Woburn, MA, USA). DNA were cloned into expression vector pET3a and sequenced to confirm that no secondary mutation had occurred. Proteins were over-expressed in *Escherichia coli* strain C41 (DE3) from Novagen (EMD Chemicals Inc., Gibbstown, NJ, USA) in LB medium. Bacterial cells were grown in 37°C until OD600 reached 0.4–0.6 and 0.4 mM isopropyl β-D-1-thiogalactopyranoside (IPTG) was added to induce protein expression at 25°C. The cells were harvested after overnight culture by

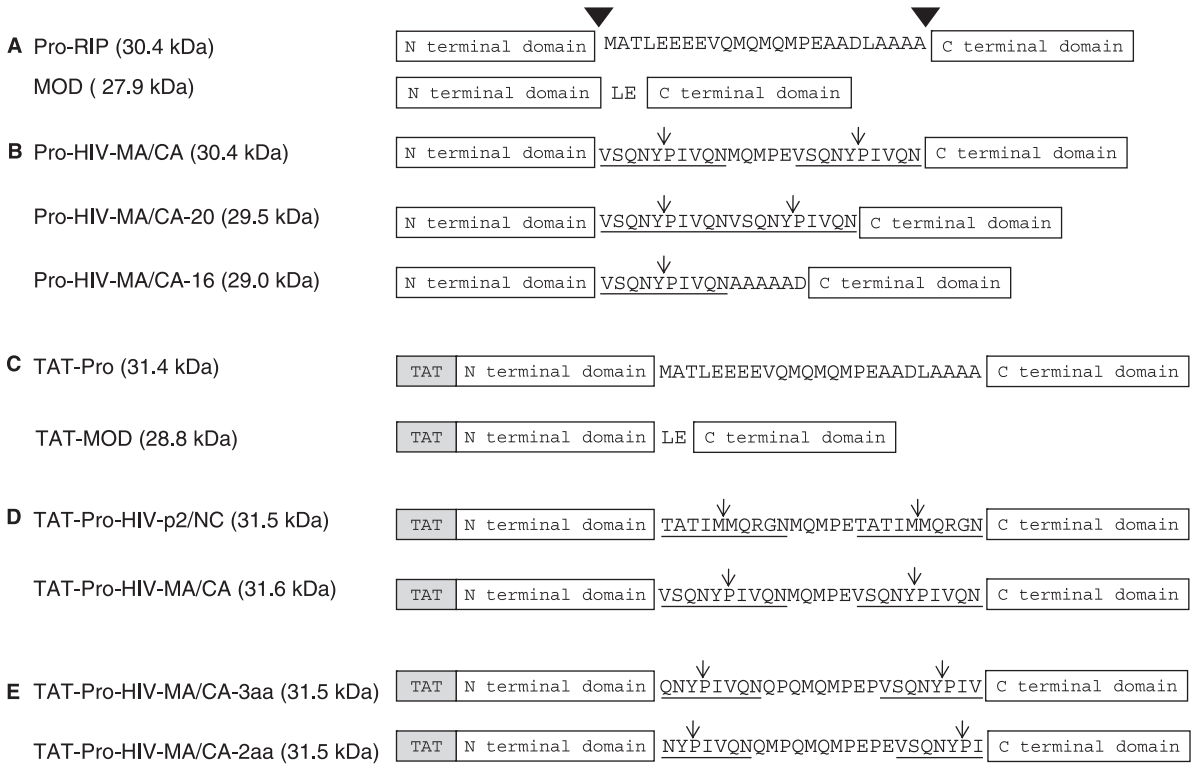

Figure 1. Schematic diagram of the maize RIP and recombinant variants. (**A**) The artificial construct maize RIP precursor Pro-RIP (Pro-RIP) contains the 25 aa internal inactivation region but without the 16 aa N-terminal and 14 aa C-terminal sequences of the inactive maize RIP precursor. The amino acid sequence of the internal inactivation region is shown. Cleavage sites leading to the generation of the active two-chain maize RIP are indicated by inverted filled triangles. MOD is another artificial construct with the two polypeptides fused by an Leu-Glu bipeptide. (**B**) The internal inactivation region was replaced by HIV-1 protease recognition site. Pro-HIV-MA/CA: the first and last 10 aa of the internal inactivation region were replaced by the 10 aa MA/CA site. Pro-HIV-MA/CA-20: two 10 aa MA/CA sites were introduced to the internal inactivation region. Pro-HIV-MA/CA-16: the whole internal inactivation region was replaced by one copy of MA/CA site followed by a hexapeptide of AAAAAD. (**C**) TAT-Pro and TAT-MOD: A Tat sequence was fused to the N-termini of Pro-RIP and MOD, respectively. (**D**) TAT-Pro-HIV-p2/NC and TAT-Pro-HIV-MA/CA: TAT-Pro with the first and last 10 aa replaced by the p2/NC site (TATIM/MQRGN) and the MA/CA site (VSQNY/PIVQN), respectively. (**E**) TAT-Pro-HIV-MA/CA-2aa and TAT-Pro-HIV-MA/CA-3aa: the recognition sequence of the MA/CA site was shortened to reduce the number of aa left to 2 and 3, respectively, after cleavage. The underlined sequences are the recognition sites of HIV-1 protease and ↓ indicates the HIV-1 protease cleavage site.

centrifugation at 4°C. For non TAT-fusion variants, cell pellet was resuspended and sonicated in 20 mM sodium phosphate buffer, pH 7.0. After centrifugation at 4°C, the supernatant was loaded to a HiTrap CM-FF column (5 ml; GE Healthcare). Protein was eluted using a linear gradient of 0–1 M NaCl in 20 mM sodium phosphate buffer, pH 7.0. The target fractions were pooled and then loaded onto a HiTrap SP XL column (5 ml; GE Healthcare). Elution was done by using a linear gradient 0–1 M NaCl in 20mM sodium phosphate buffer, pH 7.0. For TAT-fused proteins, cell pellet was resuspended and sonicated in 50 mM sodium acetate buffer, 100 mM NaCl and 8 M urea, pH 5.5 (Buffer A). The cell lysate was centrifuged at 4°C and the supernatant was loaded onto a HiTrap SP FF column (5 ml; GE Healthcare) pre-equilibrated with buffer A. Protein was eluted using a gradient of 0–1 M NaCl in 50 mM sodium acetate buffer, pH 5.5. Fractions containing the target protein were pooled and dialyzed against 50 mM sodium acetate buffer, 100 mM NaCl, 4 M urea, pH 5.5 (Buffer C) and loaded onto a HiTrap SP XL column (5 ml; GE Healthcare) pre-equilibrated with buffer C. Proteins were eluted using a linear gradient of 0–1 M NaCl in 50 mM sodium acetate buffer, pH 5.5. Target fractions were pooled and concentrated to 5 ml for further purification by a HiPrep 26/10 desalting column (GE Healthcare) pre-equilibrated with 10 mM Tris–HCl, 1 mM EDTA, 10% glycerol, pH 7.0. The purified protein was concentrated and stored at −70°C.

HIV-1 protease expression and purification

A plasmid containing the open reading frame of HIV-1 protease was provided by Prof. C.C. Wan. HIV-1 protease was then cloned into expression vector pET3b and used to transform *E. coli* BL21 (DE3) pLysS. A single colony was inoculated to 1 l of LB broth containing 100 μg/ml of ampicillin and chloramphenicol, respectively. The bacterial culture was incubated at 37°C with shaking at 250 r.p.m., until OD600 reached 0.3–0.5 and 0.4 mM IPTG was added to induce protein expression at 37°C for 4 h. HIV-1 protease was expressed as inclusion bodies and was purified as described (24).

Purification of HIV-1 protease-cleaved maize RIP variants

Purified TAT-Pro-HIV-MA/CA and TAT-Pro-HIV-p2/NC (100 μM) were incubated with recombinant HIV-1 protease (0.5 μg) in 50 mM sodium acetate buffer (pH 5.5) at 37°C for 16 h to remove the internal inactivation region. HIV-1 protease was then isolated from the activated variants by gel filtration chromatography using Superdex 75 column (GE Healthcare) which was pre-equilibrated with 10 mM Tris–HCl, 1 mM EDTA, 10% glycerol, pH 7.0. The purified variants were concentrated and stored at −70°C.

Virus and cell lines

Human T lymphocyte cell line (C8166) was obtained from Medical Research Council, AIDS Reagent Project, UK and maintained in RPMI-1640 medium (Invitrogen, Carlsbad, CA, USA) supplemented with 10% fetal bovine serum (FBS). Mouse macrophage cells (J774A.1) were purchased from American Type Culture Collection (ATCC; Manassas, VA, USA) and cultured in Dulbecco's modified Eagle's medium (Invitrogen) with 10% FBS. HIV-1_{IIIB} and HIV-1 RF/V82F/I84V were obtained from the culture supernatant of H9/HIV-1_{IIIB} and MT-2/HIV-1 RF/V82F/I84V cells, respectively. The 50% HIV-1 tissue culture infection dose ($TCID_{50}$) in C8166 cells was determined and calculated by the Reed and Muench method (25). Virus stocks were stored in aliquots at −70°C. The titre of the virus stock was 3.4×10^6 $TCID_{50}$ per millilitre (26).

N-glycosidase activity assay

Human T lymphocytes (C8166) and mouse macrophage cells (J774A.1; 1×10^6 per dish) were plated in tissue culture dishes (60 × 15 mm). Protein samples (5 μM) were added and incubated for 6 h. After incubation, culture medium was removed and the cells were washed twice by ice-cold PBS.

RNA was isolated from the treated cells using the modified TRIZOL RNA isolation protocol (27). RNA was dissolved in diethypyrocarbonate (DEPC) water and stored at −80°C and reverse-transcribed using SuperScript II Reverse Transcriptase kit (Invitrogen). RNA samples (5 μg) were prepared to a final volume of 11 μl and cDNA was synthesized at 42°C for 50 min in a final volume of 20 μl using 1 μl of Superscript II reverse transcriptase (200 U/μl). The cDNA samples were stored at −20°C.

Quantitative real-time PCR (qRT-PCR) was performed using a 7500 Fast Real-Time PCR System (Applied Biosystems) with Power SYBR Green PCR Master Mix kit (Applied Biosystems). The 20 μl reaction contained 1 μl of cDNA sample which was diluted by 100-fold from the reverse transcription reaction. Published primers were used to quantify the total 28S rRNA (control)—forward primer 5′-GATGTCGGCTCTTCCTATCATTG T-3′ and reverse primer 5′-CCAGCTCACGTTCCCTAT TAGTG-3′; and deadenylated rRNA (test)—forward primer 5′-TGCCATGGTAATCCTGCTCAGTA-3′ and reverse primer 5′-TCTGAACCTGCGGTTCCACA-3′ (28). Amplification conditions were as follows: 1 cycle at 95°C for 5 min followed by 40 cycles at 95°C for 10 sec and at 60°C for 30 sec. Each cDNA sample was run in duplication with both primer sets. Sequence Detection Software for the 7500 Fast System was used for data collection and threshold cycle (C_T) examination. Data manipulations were carried out using Prism (GraphPad Software, Inc., La Jolla, CA, USA). The C_T value of each run was converted to the amount of nucleic acid (2^{-CT}). The relative amount of altered rRNA was calculated as the amount of nucleic acid determined by the test primers divided by the amount determined by the control primers. The relative *N*-glycosidase activity was calculated as the relative amount of altered rRNA of sample-treated cells over the untreated cells. Mean ± SEM was calculated for the graphic presentation. Unpaired *t*-test was performed for statistical analysis.

Cytotoxicity assay

Cell viability was evaluated by a colorimetric method (3-(4,5-dimethylthiazol-2-yl)-2,5-diphenyltetrazoliumbromide, MTT assay) (29). Human T cells (C8166) were proliferated at log phase in RPMI-1640 medium supplemented with 10% FBS before seeded on 96 well plates (3×10^4 cell/ well, 100 µl). Six different concentration of proteins were diluted in 100 µl RPMI-1640 medium with 10% FBS and then added into the wells. After incubating at 37°C for 72 h in 5% CO_2, cells were exposed to MTT (5 mg/ml) for 4 h. To dissolve the purple formazan, 100 µl of 50% dimethylformamide and 10% SDS was added. $OD_{595/630}$ values were measured using Bio-Tek ELx 800 ELISA reader. The cell viability after treatment with different proteins was presented in percentage to control as mean ± SD and two-way ANOVA with Bonferroni test as the *post hoc* test for multiple comparison was used.

Detection of the removal of the inactivation loop

Purified protein samples (100 µM) were incubated with recombinant HIV-1 protease (0.5 µg) in 50 mM sodium acetate buffer (pH 5.5) at 37°C. Aliquot (5 µl) was collected after a 24 h incubation. The reactions were stopped by adding 5 × loading buffer and heating at 95°C for 5 min. Proteins of each reaction were analysed by SDS-PAGE. To detect cleavage of the internal inactivation region in HIV-infected cells, HIV-1_{IIIB} acutely infected human C8166 cells (1×10^6/ml) were incubated with maize RIP variants (0.2 mg/ml) at 37°C for 72 h before the isolation of cytoplasmic proteins. The cells were washed thoroughly with 5 ml ice-cold PBS twice before trypsinized at 37°C for 10 min. Cell pellets were then washed with 5 ml ice-cold PBS and then resuspended and lysed in 200 µl modified RIPA buffer (20 mM Tris–HCl, pH 7.5, 150 mM NaCl, 1 mM EDTA, 1 mM EGTA, 1% NP40, 1% sodium deoxycholate and 1 mM Na_3VO_4) with 1 mM PMSF. Cytoplasmic proteins were isolated from cell debris by centrifugation at 13 000 r.p.m., 4°C for 15 min. Supernatant (10 µl) was collected for western blot analysis. In brief, the resolved proteins were transferred from gel to polyvinylidene difluoride membrane by semi-dry transfer at 10 mA for 30 min in transfer buffer. The membrane was immediately placed into blocking buffer (5% non-fat dry milk, 10 mM Tris pH 7.5, 100 mM NaCl and 0.1% Tween 20). Anti-MOD polyclonal antibody was diluted 1:10 000 in 5 ml blocking buffer and incubated with the membrane overnight at 4°C. The membrane was then washed with wash buffer (1 × TBS buffer with 0.1% Tween 20) for three times. The secondary antibody (anti-rabbit IgG; Santa Cruz Biotechnology, Inc.) was diluted 1:5000 and incubated with agitation with the membrane at room temperature for 1 hr. Protein bands were detected by chemiluminescent (Amersham ECL western blotting detection reagents and analysis system, GE Healthcare). The blot was exposed to X-ray film (Super HR-T 30, Fujifilm) for 15–60 sec and the film was then developed.

Syncytium reduction assay

C8166 cells (3×10^4 cells/well) were seeded and inoculated with 100 $TCID_{50}$ HIV-1_{IIIB} or HIV-1 RF/V82F/I84V. Six different concentration of protein samples in 100 µl RPMI-1640 medium with 10% FBS were added to the cells and then incubated at 37°C in a humidified incubator with 5% CO_2 for 72 h. Control experiment was performed without the tested protein in HIV-1-infected and -uninfected cultures. The number of syncytia in each well was counted under microscope. Percentage inhibition of syncytial cell formation was calculated from the syncytial cell number in treated culture versus that from the uninfected control culture (26). Two-way ANOVA with Bonferroni test as the *post hoc* test for multiple comparison was used for statistical analysis.

ELISA for HIV-1 p24 antigen

HIV-1 p24 antigen in cell-free medium was measured using capture ELISA as described previously (30). Briefly, 96 well plates were coated with McAb p5F1 followed by blocking with 5% skim milk. Then, Triton X-100-treated cell-free culture medium was added and incubated at 37°C for 2 h. The plates were then incubated with diluted human polyclonal anti-HIV-1 sera, followed by HRP-labelled goat anti-human IgG and o-phenylenediamine dihydrochloride (OPD) substrate. The plates were read by Bio-Tek ELx 800 ELISA reader at 490/630 nm within 30 min after the reaction. The inhibition percentage of p24 antigen expression was calculated in comparison with the uninfected control culture. Two-way ANOVA with Bonferroni test as the *post hoc* test for multiple comparison was used for statistical analysis. The concentration of protein that caused a reduction of p24 antigen expression by 50% (EC_{50}) was determined from the dose-response curve.

RESULTS

Specific cleavage of HIV-1 protease-sensitive maize RIP variants *in vitro* and in HIV-infected cells

The HIV-1 protease cleavage sequences TATIM/MQRGN (p2/NC site) and VSQNY/PIVQN (MA/CA site) located in the polyprotein precursor Gag of HIV-1 (31) were selected based on their high k_{cat}/K_m values towards HIV-1 protease (32,33). We first replaced the whole internal inactivation region by two consecutive MA/CA sites. However, the variant Pro-HIV-MA/CA-20 could only be partially cleaved by HIV-1 protease (Figures 1B and 2A). Shortening the internal inactivation region by changing the C-terminal MA/CA site to a hexapeptide AAAAAD resulted in an uncleavable variant (Pro-RIP-MA/CA-16; Figures 1B and 2A). We then kept the length of the internal inactivation region (25 aa) and replaced the first and the last 10 aa with the MA/CA site (Figure 1B). This Pro-RIP-MA/CA variant was cleaved completely by HIV-1 protease into two target bands (~11 kDa and 17 kDa) in 16 h at 37°C (Figure 2A).

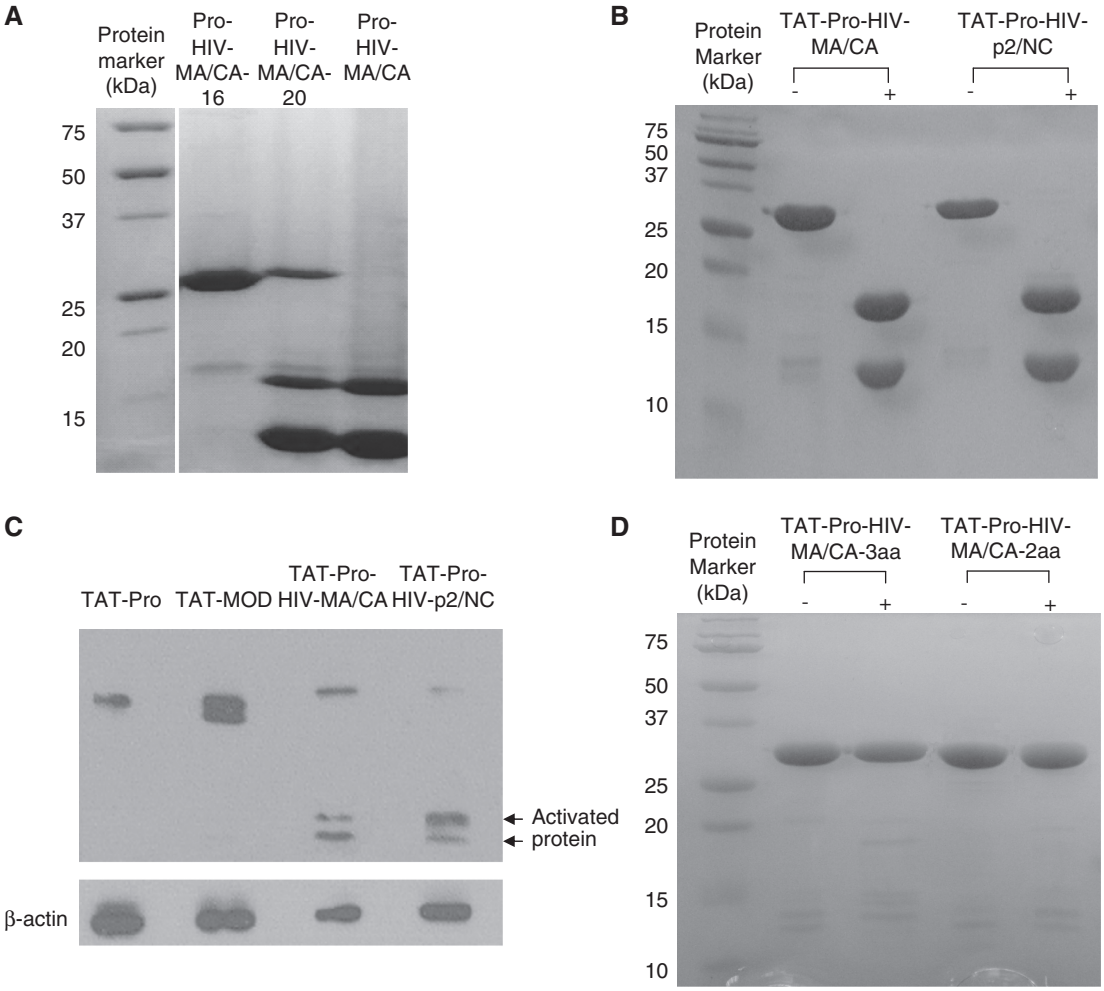

Figure 2. Cleavage of TAT-fused maize RIP variants by HIV-1 protease. (**A**) Pro-HIV-MA/CA-16, Pro-HIV-MA/CA-20 and Pro-HIV-MA/CA were cleaved by purified recombinant HIV-1 protease *in vitro*. Only Pro-HIV-MA/CA was completely cleaved. (**B**) TAT-Pro-HIV-MA/CA and TAT-Pro-HIV-p2/NC were completely cleaved by HIV-1 protease *in vitro*. (**C**) HIV-1_{IIIB} acutely infected C8166 cells (1×10^6) were incubated with protein samples (0.4 μg in a volume of 2 ml) for 72 h and immunoblotted with anti-MOD polyclonal antibodies specific for Pro-RIP and its cleavage fragments (~11 and 17 kDa). (**D**) TAT-Pro-HIV-MA/CA-3aa and TAT-Pro-HIV-MA/CA-2aa were not cleaved by the same *in vitro* cleavage reaction condition as in (A) and (B). Proteins were resolved by 15% SDS gel.

To promote cell entry, an 11 aa transduction peptide YGRKKRRQRRR derived from the HIV-1 Tat protein was fused to the N-termini of Pro-RIP and MOD to generate TAT-Pro and TAT-MOD, respectively (Figure 1C). The two TAT-fused maize RIP variants TAT-Pro-HIV-p2/NC and TAT-Pro-HIV-MA/CA with the substitution of HIV-1 protease recognition sequences TATIM/MQRGN (p2/NC site) and VSQNY/PIVQN (MA/CA site), respectively, in the 25 aa internal inactivation region (Figure 1D) were cleaved by HIV-1 protease under the same conditions of the non-TAT variants (Figure 2B). Thus, fusion of the TAT transduction peptide did not affect the cleavage efficiency *in vitro*. In addition, western blot analysis indicated that these TAT-fused variants were also cleaved inside the HIV-1_{IIIB} acutely infected C8166 cells (Figure 2C). No detectable proteolytic cleavage by HIV-1 protease was observed for TAT-Pro (Figure 2C). Attempts to shorten the extra aa in the cleaved products by eliminating two or three of the amino acid residues from the MA/CA site (Figure 1E), resulted in uncleavable variants (TAT-Pro-HIV-MA/CA-3aa and TAT-Pro-HIV-MA/CA-2aa; Figure 2D).

Enzymatic activity assay for cleaved TAT-fused maize RIP

To compare the *N*-glycosidase activity of the maize RIP variants before and after the removal of the internal inactivation region, HIV-1 protease-cleaved TAT-Pro-HIV-MA/CA and TAT-Pro-HIV-p2/NC were purified by gel filtration chromatography and incubated with mouse macrophages (J774A.1) for 6 h. Afterwards, total RNA was isolated for cDNA synthesis. The amount of rRNA depurination was detected quantitatively in a site-specific manner using primers that targeted the altered sequences by qRT-PCR (28). Two published primer sets were used for the amplification of the total 28S rRNA and the depurinated site caused by the *N*-glycosidase activity, respectively (28). The efficiency of the primer sets was tested using serial dilution of cDNA synthesized from the total

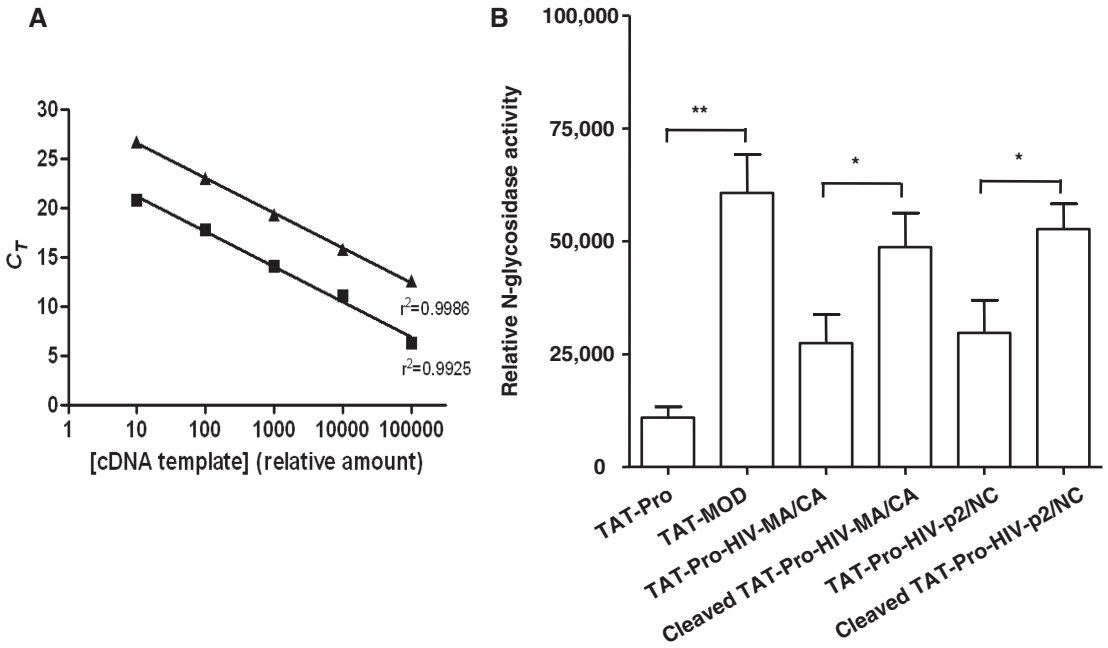

Figure 3. *In vivo N*-glycosidase activity of TAT-fused maize RIP and variants in mouse macrophage 28S rRNA (J774A.1). During first-strand cDNA synthesis, reverse transcriptase preferentially inserts an adenine at the site of depurination, resulting in a T to A transversion in sequencing reads. *N*-glycosidase activity was determined by qPCR using primers that target the modified site. (**A**) qRT-PCR efficiency test for primer pairs. Signals were obtained from the amplification of serially diluted cDNA synthesized from the RNA of TAT-MOD treated cells. Filled square indicates total 28S rRNA and filled triangle indicates depurinated rRNA. The relative amount of cDNA template was plotted against the corresponding threshold cycle number in log scale and fitted with a linear regression model. SEMs were less than 1% of the corresponding C_T values. (**B**) Relative *N*-glycosidase activity of the TAT-fused maize RIP and variants. The relative *N*-glycosidase activity was calculated as the relative amount of altered rRNA of sample-treated cells over the untreated cells and mean ± SEM was calculated for the graphic presentation. Unpaired *t*-test was performed for statistical analysis ($n = 6$) ($^*P < 0.05$, $^{**}P < 0.01$).

RNA of TAT-MOD treated cells. Figure 3A shows the linearity of the standard curves throughout the whole range of serial dilution ($r^2 > 0.99$). The relative *N*-glycosidase activity of TAT-MOD was about 5.5-fold higher than TAT-Pro in mouse macrophage cells (J774A.1; Figure 3B). Incubation with the cleaved variants (cleaved TAT-Pro-HIV-MA/CA and cleaved TAT-Pro-HIV-p2/NC) also resulted in a higher level of depurinated rRNA than their uncleaved counterparts in mouse macrophages (Figure 3B). This showed that cleavage at the modified internal inactivation region by HIV-1 protease restored the *N*-glycosidase activity.

Anti-HIV activity and *N*-glycosidase activity in HIV-1 infected cells

TAT-Pro and TAT-MOD were tested for the inhibition of HIV replication in human T cells (C8166) infected with two HIV-1 strains, HIV-1_{IIIB} and an HIV-1 protease inhibitor-resistant virus strain, (HIV-1 RF/V82F/I84V). The latter strain is among the most commonly observed in patients receiving protease inhibitor-containing regimens (34,35). In HIV-1_{IIIB} acutely infected C8166 cells, TAT-MOD showed concentration-dependent inhibition of HIV replication. The 50% inhibition of syncytium and p24 antigen production were at 0.62 ± 0.08 μM and 0.21 ± 0.02 μM (mean ± SD in three experiments), respectively (Table 1). In HIV-1 RF/V82F/I84V acutely infected C8166 cells treated with TAT-MOD, the 50% inhibition on syncytium and p24 antigen production were at 0.37 ± 0.05 μM and 0.23 ± 0.03 μM (mean ± SD in three experiments), respectively. TAT-Pro had a weaker inhibitory effect on p24 antigen production with IC_{50} 1.20 ± 0.25 μM and 10.87 ± 5.13 μM in HIV-1_{IIIB} and HIV-1 RF/V82F/I84V acutely infected C8166 cells, respectively (Table 1 and Supplementary Figure S1).

The anti-HIV activities of TAT-Pro-HIV-MA/CA and TAT-Pro-HIV-p2/NC towards HIV-infected cells, as well as the cytotoxic effects towards uninfected cells were examined. TAT-MOD and variants TAT-Pro-HIV-MA/CA and TAT-Pro-HIV-p2/NC were potent in inhibiting syncytium formation and p24 antigen production in HIV-1_{IIIB} and HIV-1 RF/V82F/I84V acutely infected C8166 cells, whereas TAT-Pro possessed limited inhibitory effects (Table 1 and Supplementary Figure S1). We found that the relative *N*-glycosidase activity of TAT-MOD and the two variants were statistically comparable in HIV-1_{IIIB} acutely infected C8166 (Figure 4), functionally showing that the variants indeed went through an activation process by endogenous HIV-1 protease *in vivo*. In addition, a smaller amount of depurinated rRNA was detected in uninfected C8166 cells treated with the variants compared with TAT-MOD-treated cells (Figure 4). Compared to TAT-MOD, the two variants were at least 5-fold less cytotoxic towards uninfected C8166 cells (Table 1). It suggested that this HIV-1 protease-activation mechanism enhanced the specificity of maize RIP towards HIV-1 infected cells without compromising its *N*-glycosidase activity.

Table 1. Cytotoxicity of TAT-fused maize RIP variants in uninfected C8166 cells and inhibition of viral replication in HIV-1_{IIIB} and HIV-1 RF/V82F/184V acutely infected C8166 cells

	Uninfected C8166	HIV-1_{IIIB}		HIV-1 RF/V82F/I84V	
	Cytotoxicity IC_{50} (μM)	Syncytial reduction EC_{50} (μM)	p24 antigen reduction EC_{50} (μM)	Syncytial reduction EC_{50} (μM)	p24 antigen reduction EC_{50} (μM)
TAT-Pro	>15.93	5.69 ± 0.96	1.20 ± 0.25	6.02 ± 0.67	10.87 ± 5.13
TAT-MOD	3.27 ± 0.26	0.62 ± 0.08	0.21 ± 0.02	0.37 ± 0.05	0.23 ± 0.03
TAT-Pro-HIV-p2/NC	>15.87	0.55 ± 0.05	0.19 ± 0.02	0.33 ± 0.01	0.15 ± 0.03
TAT-Pro-HIV-MA/CA	>15.78	1.27 ± 0.15	0.57 ± 0.17	1.71 ± 0.13	1.30 ± 0.33

The values are means ± SD of three experiments ($n = 12$).

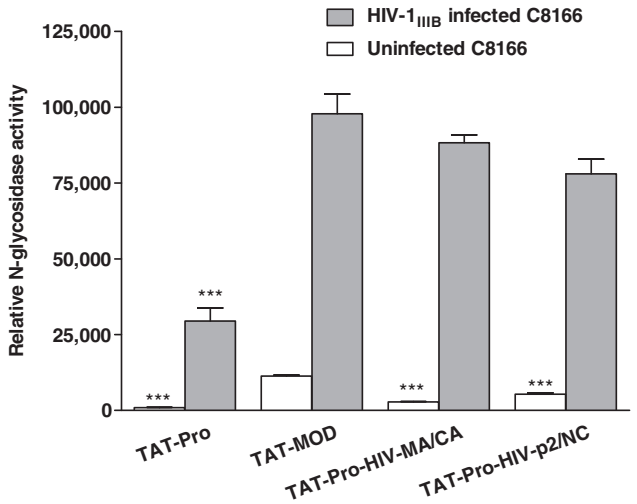

Figure 4. *N*-glycosidase activity of TAT-fused maize RIP and variants in uninfected and HIV-1_{IIIB} acutely infected human T lymphocyte C8166 cells. Relative *N*-glycosidase activity was represented in linear scale ± SEM. Grey bars indicate HIV-1_{IIIB} acutely infected C8166 cells, while white bars indicate uninfected cells. Student *t*-test was used for statistical analysis. $^{***}P < 0.001$ versus TAT-MOD ($n = 6$).

DISCUSSION

We have recently solved the crystal and solution structures of maize RIP (4,5). Except for the presence of an internal inactivation region (Ala163-Asp189) on the surface of the inactive precursor (Pro-RIP), the structures of Pro-RIP and the one-chain active form (MOD) are highly similar, indicating that the removal of the internal inactivation region does not alter the global structure of maize RIP. Several studies suggested that RIPs get access to the ribosome by interacting with ribosomal proteins. Trichosanthin has been shown to bind to ribosomal proteins P0, P1 and P2 (36,37) and PAP to L3 (38,39). It has also been reported that an α-helix at the C-terminal domain of trichosanthin is responsible for binding to P2 (36). By NMR chemical shift perturbation, the P2 binding site of MOD has been mapped to the N-terminal domain near the internal inactivation region, which has four positively charged residues (K143–K146) (5). The 25 aa internal inactivation region is believed to sterically hinder the interaction of Pro-RIP with the ribosome, as pull down assay has shown that Pro-RIP cannot interact with rat ribosome and surface plasmon resonance analysis showed that the dissociation constant (K_D) of Pro-RIP on purified rat ribosome is about 80-fold higher than that of MOD (4).

With the knowledge of its role, we consider this inactivation region a unique opportunity for targeting maize RIP towards cells that express a specific protease for cleaving the region. First, we established that replacing the first and last 10 amino acid residues of the internal inactivation region with the 10 aa MA/CA or p2/NC HIV-1 protease cleavage site (Figure 1C) resulted in specific cleavage *in vitro* and in HIV-infected cells (Figure 2A and B). Then we showed that the TAT-fusion maize RIP variants exhibited higher inhibitory effects on p24 and syncytium formation in HIV-1 infected human C8166 and lower cytotoxic effects in uninfected cells. This demonstrated the possibility of using the internal inactivation region of maize RIP as a switch to activate the cytotoxin inside the target cells.

Studies of the MA/CA site using synthetic peptides suggested that the residues occupying position P4 through P3′ flanking the scissile bonds were critical for specific and efficient cleavage (31,40). In our hands, however, variant TAT-Pro-HIV-MA/CA-3aa which had the MA/CA sites QNY/PIVQN (P3 to P5′) and VSQNY/PIV (P5 to P3′) within a 25 aa sequence was not cleaved by HIV-1 protease *in vitro*, suggesting that the maize RIP sequence immediately next to the protease sites also play a role in the cleavage efficiency. Our data also suggested that the length of the internal inactivation region is important for the access of the HIV-1 protease. We found that restoring the length to the naturally occurred internal region (25 aa) resulted in efficient HIV-1 protease cleavage. Variants Pro-HIV-MA/CA-16 and Pro-HIV-MA/CA-20 with 16 and 20 aa internal inactivation region resulted in incomplete cleavage. In addition, different HIV-1 protease cleavage sites were cleaved in different efficiency. Compared to TAT-Pro-HIV-MA/CA, the higher inhibitory activity of TAT-Pro-HIV-p2/NC on the replication of HIV-1_{IIIB} and HIV-1 RF/V84F/I84V (Table 1) is probably due to a more efficient *in vivo* cleavage of the p2/NC site. It has been reported that after translation of the HIV Gag precursor, initial cleavage occurred at the p2/NC site which releases the RNA-binding NC protein followed by an intermediate rate of cleavage at the

MA/CA (31,41–43). The order of cleavage has been shown to be p2/NC > p1/p6 ≥ MA/CA >CA/p2 *in vitro* (44).

Traditionally, *N*-glycosidase activity was assayed indirectly by cell-free protein synthesis inhibition (45) or directly by colorimetric detection of released adenine by high performance liquid chromatography (HPLC) (46). These methods suffer from low sensitivity and specificity, and can only measure the *in vitro N*-glycosidase activity. To achieve the high specificity and sensitivity required for measuring the *in vivo N*-glycosidase activity of the internalized maize RIP variants, the approach developed by Melchior and Tolleson (28) was used to directly measure the amount of depurinated rRNA. Our results showed that the HIV-1 protease-activated variants had an increased *N*-glycosidase activity compared to their uncleaved counterparts in mouse macrophages (Figure 3B). The maize RIP variants indeed possess catalytic function in cells.

Our observation on the *N*-glycosidase activity of TAT-MOD and TAT-Pro indicated that the removal of the internal inactivation region increases the cytotoxicity and anti-HIV activity of maize RIP (Table 1). The relative *N*-glycosidase activity of TAT-MOD in HIV-1_{IIIB} acutely infected C8166 cells was about 5-fold higher than that of the TAT-Pro and the results were consistent with the same assay using mouse macrophage J774A.1 (Figures 3B and 4). Similarly, by comparing the EC_{50} of inhibition of p24 antigen production in HIV-1_{IIIB} and HIV-1 RF/V82F/I84V infected cells to TAT-Pro, the HIV-1 protease-cleavable variants TAT-Pro-HIV-MA/CA and Pro-TAT-Pro-HIV-p2/NC had 2- to 70-fold increase in the inhibitory power while showing low cytotoxicity towards uninfected C8166 cells. The data showed that compared to the *N*-glycosidase activity, HIV replication is more sensitive to the activated maize RIP variants. The next step for generating a useful anti-HIV agent is to test the effect of these variants in an HIV-infected animal model and to further improve their specificity and activity.

HIV-1 protease recognition sites have been employed by other groups for the development of anti-HIV agents. Serio and co-workers (47,48) demonstrated that the introduction of an HIV protease cleavage site into the C-terminus of Vpr inhibited the infectivity of HIV-1 provirus, because of the incomplete processing of the polyprotein for viral maturation. Vocero-Akbani and co-workers (49) modified a protease-activated caspase-3 by placing an HIV-1 protease cleavage site between its p17 and p12 domains, where a 5 aa cleavage sequence (IETD↓S) was originally located between these domains in the wild-type caspase-3 inactive precursor. This modified caspase-3 induced apoptosis in Jurkat T cells co-transduction with HIV protease (50). However, it is not known whether the caspase was cleaved efficiently to cause specific killing of the HIV-infected cells. Mitrea and co-workers (51) inserted an HIV-1 protease recognition sequence into a surface loop of barnase and confirmed that it can be cleaved by HIV protease *in vitro*. However, there has been no study of its catalytic activity in the cells.

Here, we have demonstrated that by incorporating the HIV-1 protease cleavage sites to the internal inactivation region, we can generate modified maize RIP with cytotoxicity switched on by HIV-1 protease inside HIV-1 infected cells. The variants had reduced cytotoxicity towards uninfected cells, but exhibited potent anti-HIV activity in HIV-infected cells. The switching mechanism described here provides a technology platform for creating pathogen-specific cytotoxins. By incorporating different pathogen-specific protease target sites into the internal inactivation region, maize RIP in principle can be activated inside and destroy the concerned cells. Since different RIPs possess similar 3D structures, a modified inactivation region may also be added to other RIPs for targeting cells infected by HIV or other pathogens.

SUPPLEMENTARY DATA

Supplementary Data are available at NAR Online.

ACKNOWLEDGEMENTS

Thanks are due to Prof. R.S. Boston of North Carolina State University for the clones of maize RIP and Prof. C.C. Wan of the Chinese University of Hong Kong for the clone of HIV-1 protease.

FUNDING

For work in Hong Kong: Research Grants Council of Hong Kong SAR (CUHK4606/06M); University Grants Council of Hong Kong SAR One-Off Special Equipment Grant (SEG CUHK08). For work in Kunming: 973 Program (2009CB522306); CAS (KSCX1-YW-R-24); Key Scientific and Technological projects of China (2009ZX09501-029, 2008ZX10001-015, 2008ZX10005-005). Funding for open access charge: Department of Biochemistry; The Chinese University of Hong Kong.

Conflict of interest statement. None declared.

REFERENCES

1. Bass,H.W., Krawetz,J.E., Obrain,G.R., Zinselmeier,C., Habben,J.E. and Boston,R.S. (2004) Maize ribosome-inactivating proteins (RIPs) with distinct expression patterns have similar requirements for proenzyme activation. *J. Exp. Bot.*, **55**, 2219–2233.
2. Hey,T.D., Hartley,M. and Walsh,T.A. (1995) Maize ribosome-inactivating protein (b-32): homologs in related species, effects on maize ribosomes, and modulation of activity by pro-peptide deletions. *Plant Physiol.*, **107**, 1323–1332.
3. Walsh,T.A., Morgan,A.E. and Hey,T.D. (1991) Characterization and molecular cloning of a proenzyme form of a ribosome-inactivating protein from maize. *J. Biol. Chem.*, **266**, 23422–23427.
4. Mak,A.N., Wong,Y.T., An,Y.J., Cha,S.S., Sze,K.H., Au,S.W., Wong,K.B. and Shaw,P.C. (2007) Structure-function study of maize ribosome-inactivating protein: implications for the internal inactivation region and the sole glutamate in the active site. *Nucleic Acids Res.*, **35**, 6259–6267.
5. Yang,Y., Mak,A.N., Shaw,P.C. and Sze,K.H. (2010) Solution structure of an active mutant of maize ribosome-inactivating protein (MOD) and its interaction with the ribosomal stalk protein P2. *J. Mol. Biol.*, **395**, 897–907.

6. Yang,Y., Mak,A.N., Shaw,P.C. and Sze,K.H. (2007) (1)H, (13)C and (15)N backbone and side chain resonance assignments of a 28 kDa active mutant of maize ribosome-inactivating protein (MOD). *Biomol. NMR Assign.*, **1**, 187–189.
7. Leung,K.N., Yeung,H.W. and Leung,S.O. (1986) The immunomodulatory and antitumor activities of trichosanthin-an abortifacient protein isolated from tian-hua-fen (Trichosanthes kirilowii). *Asian Pac. J. Allergy Immunol.*, **4**, 111–120.
8. Maraganore,J.M., Joseph,M. and Bailey,M.C. (1987) Purification and characterization of trichosanthin. Homology to the ricin A chain and implications as to mechanism of abortifacient activity. *J. Biol. Chem.*, **262**, 11628–11633.
9. Abuharbeid,S., Apel,J., Sander,M., Fiedler,B., Langer,M., Zuzarte,M.L., Czubayko,F. and Aigner,A. (2004) Cytotoxicity of the novel anti-cancer drug rViscumin depends on HER-2 levels in SKOV-3 cells. *Biochem. Biophys. Res. Commun.*, **321**, 403–412.
10. Citores,L., Ferreras,J.M., Muñoz,R., Benítez,J., Jiménez,P. and Girbés,T. (2002) Targeting cancer cells with transferrin conjugates containing the non-toxic type 2 ribosome-inactivating proteins nigrin b or ebulin I. *Cancer Lett.*, **184**, 29–35.
11. Geden,S.E., Gardner,R.A., Fabbrini,M.S., Ohashi,M., Phanstiel Iv,O. and Teter,K. (2007) Lipopolyamine treatment increases the efficacy of intoxication with saporin and an anticancer saporin conjugate. *FEBS J.*, **274**, 4825–4836.
12. Lee-Huang,S., Huang,P.L., Kung,H.F., Li,B.Q., Huang,P.L., Huang,P., Huang,H.I. and Chen,H.C. (1991) TAP29: an anti-human immunodeficiency virus protein from Trichosanthin kirilowii that is nontoxic to intact cells. *Proc. Natl Acad. Sci. USA*, **88**, 6570–6574.
13. Uckun,F.M., Bellomy,K., O'Neill,K., Messinger,Y., Johnson,T. and Chen,C.L. (1999) Toxicity, biological activity, and pharmacokinetics of TXU (Anti- CD7)-Pokeweed antiviral protein in chimpanzees and adult patients infected with human immunodeficiency virus. *J. Pharmacol. Exp. Ther.*, **291**, 1301–1307.
14. Uckun,F.M., Chelstrom,L.M., Tuel-Ahlgren,L., Dibirdik,I., Irvin,J.D., Langlie,M.C. and Myers,D.E. (1998) TXU (anti-CD7)-pokeweed antiviral protein as a potent inhibitor of human immunodeficiency virus. *Antimicrob. Agents Chemother.*, **42**, 383–388.
15. Kahn,J.O., Gorelick,K.J., Gatti,G., Arri,C.J., Lifson,J.D., Gambertoglio,J.G., Bostrom,A. and Williams,R. (1994) Safety, activity, and pharmacokinetics of GLQ223 in patients with AIDS and AIDS-related complex. *Antimicrob. Agents Chemother.*, **38**, 260–267.
16. Pincus,S.H., Wehrly,K., Tschachler,E., Hayes,S.F., Buller,R.S. and Reitz,M. (1990) Variants selected by treatment of human immunodeficiency virus-infected cells with an immunotoxin. *J. Exp. Med.*, **172**, 745–757.
17. Bell,K.D., Ramilo,O. and Vitetta,E.S. (1993) Combined use of an immunotoxin and cyclosporine to prevent both activated and quiescent peripheral blood T cells from producing type 1 human immunodeficiency virus. *Proc. Natl Acad. Sci. USA*, **90**, 1441–1445.
18. Shaw,P.C., Lee,K.M. and Wong,K.B. (2005) Recent advances in trichosanthin, a ribosome-inactivating protein with multiple pharmacological properties. *Toxicon*, **45**, 683–689.
19. Stirpe,F. and Battelli,M.G. (2006) Ribosome-inactivating proteins: progress and problems. *Cell Mol. Life Sci.*, **63**, 1850–1866.
20. Till,M.A., Zolla-Pazner,S., Gorny,M.K., Patton,J.S., Uhr,J.W. and Vitetta,E.S. (1989) Human immunodeficiency virus-infected T cells and monocytes are killed by monoclonal human anti-gp41 antibodies coupled to ricin A chain. *Proc. Natl Acad. Sci. USA*, **86**, 1987–1991.
21. Lee-Huang,S., Kung,H.F., Huang,P.L., Huang,P.L., Li,B.Q., Huang,P., Huang,H.I. and Chen,H.C. (1991) A new class of anti-HIV agents: GAP31, DAPs 30 and 32. *FEBS Lett.*, **291**, 139–144.
22. Zhao,W.L., Feng,D., Wu,J. and Sui,S.F. (2010) Trichosanthin inhibits integration of human immunodeficiency virus type 1 through depurinating the long-terminal repeats. *Mol. Biol. Rep.*, **37**, 2093–2098.
23. Lee-Huang,S., Kung,H.F., Huang,P.L., Bourinbaiar,A.S., Morell,L.J., Brown,J.H., Huang,P.L., Tsai,W.P., Chen,A.Y., Huang,H.I. *et al.* (1994) Human immunodeficiency virus type 1 (HIV-1) inhibition, DNA-binding, RNA-binding, and ribosome inactivating activities in the N-terminal segments of the plant anti-HIV protein GAP31. *Proc. Natl Acad. Sci. USA*, **91**, 12208–12212.
24. Lin,X.L., Lin,Y.Z. and Tang,J. (1994) Relationships of human immunodeficiency virus protease with eukaryotic aspartic proteases. *Methods Enzymol.*, **241**, 195–224.
25. Dulbecco,R. (1988) Endpoint methods–measurements of the infectious titer of a viral sample. In Dulbecco,R. and Ginsberg,H.S. (eds), *Virology*. J.P. Lippincott, Philadelphia, pp. 22–25.
26. Wang,R.R., Gu,Q., Wang,Y.H., Zhang,X.M., Yang,L.M., Zhou,J., Chen,J.J. and Zheng,Y.T. (2008) Anti HIV-1 activities of compounds isolated from the medicinal plant Rhus chinensis. *J. Ethnopharmacol.*, **117**, 249–256.
27. Chomczynski,P. and Mackey,K. (1995) Short technical reports. Modification of the TRI reagent procedure for isolation of RNA from polysaccharide- and proteoglycan-rich sources. *Biotechniques*, **19**, 942–945.
28. Melchior,W.B. Jr and Tolleson,W.H. (2010) A functional quantitative polymerase chain reaction assay for ricin, Shiga toxin, and related ribosome-inactivating proteins. *Anal. Biochem.*, **396**, 204–211.
29. Mosmann,T. (1983) Rapid colorimetric assay for cellular growth and survival: application to proliferation and cytotoxicity assays. *J. Immunol. Methods*, **65**, 55–63.
30. Zheng,Y.T., Ben,K.L. and Jin,S.W. (2000) Anti-HIV-1 activity of trichosanthin, a novel ribosome-inactivating protein. *Acta Pharmacol. Sin.*, **21**, 179–182.
31. Pettit,S.C., Henderson,G.J., Schiffer,C.A. and Swanstrom,R. (2002) Replacement of the P1 amino acid of human immunodeficiency virus type 1 Gag processing sites can inhibit or enhance the rate of cleavage by the viral protease. *J. Virol.*, **76**, 10226–10233.
32. Kádas,J., Weber,I.T., Bagossi,P., Miklóssy,G., Boross,P., Oroszlan,S. and Tözsér,J. (2004) Narrow substrate specificity and sensitivity toward ligand-binding site mutations of human T-cell Leukemia virus type 1 protease. *J. Biol. Chem.*, **279**, 27148–27157.
33. Tözsér,J., Bláha,I., Copeland,T.D., Wondrak,E.M. and Oroszlan,S. (1991) Comparison of the HIV-1 and HIV-2 proteinases using oligopeptide substrates representing cleavage sites in Gag and Gag-Pol polyproteins. *FEBS Lett.*, **281**, 77–80.
34. Klei,H.E., Kish,K.K., Lin,P.F.M., Guo,Q., Friborg,J., Rose,R.E., Zhang,Y., Goldfarb,V., Langley,D.R., Wittekind,M. *et al.* (2007) X-ray crystal structures of human immunodeficiency virus type 1 protease mutants complexed with atazanavir. *J. Virol.*, **81**, 9525–9535.
35. Shafer,R.W. (2002) Genotypic testing for human immunodecifiency virus type 1 drug resistance. *Clin. Microbiol. Rev.*, **15**, 247–277.
36. Too,P.H., Ma,M.K., Mak,A.N., Wong,Y.T., Tung,C.K., Zhu,G., Au,S.W., Wong,K.B. and Shaw,P.C. (2009) The C-terminal fragment of the ribosomal P protein complexed to trichosanthin reveals the interaction between the ribosome-inactivating protein and the ribosome. *Nucleic. Acids Res.*, **37**, 602–610.
37. Chan,S.H., Hung,F.S., Chan,D.S. and Shaw,P.C. (2001) Trichosanthin interacts with acidic ribosomal proteins P0 and P1 and mitotic checkpoint protein MAD2B. *Eur. J. Biochem.*, **268**, 2107–2112.
38. Rajamohan,F., Venkatachalam,T.K., Irvin,J.D. and Uckun,F.M. (1999) Pokeweed antiviral protein isoforms PAP-1, PAP-II, and PAP-III depurinate RNA of human immunodeficiency virus (HIV)-1. *Biochem. Biophy. Res. Commun.*, **260**, 453–458.
39. Hudak,K.A., Dinman,J.D. and Tumer,N.E. (1999) Pokeweed antiviral protein accesses ribosomes by binding to L3. *J. Biol. Chem.*, **274**, 3859–3864.
40. Bagossi,P., Sperka,T., Fehér,A., Kádas,J., Zahuczky,G., Miklóssy,G., Boross,P. and Tözsér,J. (2005) Amino acid preferences for a critical substrate binding subsite of retroviral proteases in type 1 cleavage sites. *J. Virol.*, **79**, 4213–4218.
41. Wiegers,K., Rutter,G., Kottler,H., Tessmer,U., Hohenberg,H. and Kräusslich,H.G. (1998) Sequential steps in human immunodeficiency virus particle maturation revealed by alterations

of individual Gag polyprotein cleavage sites. *J. Virol.*, **72**, 2846–2854.
42. Pettit,S.C., Clemente,J.C., Jeung,J.A., Dunn,B.M. and Kaplan,A.H. (2005) Ordered processing of the human immunodeficiency virus type 1 GagPol precursor is influenced by the context of the embedded viral protease. *J. Virol.*, **79**, 10601–10607.
43. Pettit,S.C., Lindquist,J.N., Kaplan,A.H. and Swanstorm,R. (2005) Processing sites in the human immunodeficiency virus type 1 (HIV-1) Gag-Pro-Pol precursor are cleaved by the viral protease at different rates. *Retrovirology*, **2**, 66–71.
44. Kräusslich,H.G., Ingraham,R.H., Skoog,M.T., Wimmer,E., Pallai,P.V. and Carter,C.A. (1989) Activity of purified biosynthetic proteinase of human immunodeficiency virus on natural substrates and synthetic peptides. *Proc. Natl Acad. Sci. USA*, **86**, 807–811.
45. Olsnes,S., Fernandez-Puentes,C., Carrasco,L. and Vazquez,D. (1975) Ribosome inactivation by the toxic lectins abrin and ricin. Kinetics of the enzymic activity of the toxin A-chains. *Eur. J. Biochem.*, **60**, 281–288.
46. Heisler,I., Keller,J., Tauber,R., Sutherland,M. and Fuchs,H. (2002) A colorimetric assay for the quantitation of free adenine applied to determine the enzymatic activity of ribosome-inactivating proteins. *Anal. Biochem.*, **302**, 114–122.
47. Serio,D., Rizvi,T.A., Cartas,M., Kalyanaraman,V.S., Weber,I.T., Koprowski,H. and Srinivasan,A. (1997) Development of a novel anti-HIV-1 agent from within: effect of chimeric Vpr-containing protease cleavage site residues on virus replication. *Proc. Natl Acad. Sci. USA*, **94**, 3346–3351.
48. Serio,D., Singh,S.P., Cartas,M.A., Weber,I.T., Harrison,R.W., Louis,J.M. and Srinivasan,A. (2000) Antiviral agent based on the non-structural protein targeting the maturation process of HIV-1: expression and susceptibility of chimeric Vpr as a substrate for cleavage by HIV-1 protease. *Protein Eng.*, **13**, 431–436.
49. Vocero-Akbani,A.M., Heyden,N.V., Lissy,N.A., Ratner,L. and Dowdy,S.F. (1999) Killing HIV-infected cells by transduction with an HIV protease-activated caspase-3 protein. *Nat. Med.*, **5**, 29–33.
50. Han,Z., Hendrickson,E.A., Bremner,T.A. and Wyche,J.H. (1997) A sequential two-step mechanism for the production of the mature p17:p12 form of caspase-3 in vitro. *J. Biol. Chem.*, **272**, 13432–13436.
51. Mitrea,D.M., Parsons,L.S. and Loh,S.N. (2010) Engineering an artificial zymogen by alternate frame protein folding. *Proc. Natl Acad. Sci. USA*, **107**, 2824–2829.